Interference effects in electron capture from insulator surfaces

M. S. Gravielle and J. E. Miraglia
Instituto de Astronomía y Física del Espacio (IAFE), Consejo Nacional de Investigaciones Científicas y Técnicas, Casilla de Correo 67, Sucursal 28, 1428 Buenos Aires, Argentina
and Departamento de Física, FCEN, Universidad de Buenos Aires, Buenos Aires, Argentina
(Received 1 September 2004; published 22 March 2005)

We investigate the electron capture from insulator surfaces under grazing impact conditions. The eikonal-impulse approximation is used to describe coherent electron exchange from surface ions. In the model the transition amplitude is expressed as the sum of atomic transition amplitudes, each one associated with capture from a different lattice site. The method is applied to 100 keV protons colliding on LiF surfaces. Strong interference effects as a function of the crystal orientation were found for the partial capture from a given initial crystal state. However, these interference structures disappear when the contributions from different crystal states add up to obtain the total capture probability from the surface band.

DOI: 10.1103/PhysRevA.71.032901 PACS number(s): 34.50.Dy

I. INTRODUCTION

When a fast ion interacts with a crystal surface, different interference phenomena reveal the periodic structure of the solid. In grazing collisions with solid surfaces such interference effects were observed for excitation [1,2] and ionization [3,4] of projectiles carrying bound electrons. The transition probabilities associated with these processes display oscillatory patterns, which are related to the periodic behavior of the lattice potential. Similar effects were also detected in ions channeled through crystal foils via the changes produced in the charge state of the ion [5–7] and in the electron-emission yield [8], and via x-ray emission following electronic deexcitation of the ions [9,10]. On the other hand, interference structures have been observed in ionization spectra of molecular hydrogen by ion impact [11–13], where the two atomic centers of H_2 resemble the two slits of Young's experiment.

The aim of this article is to investigate the coherent electron transitions produced by grazing scattering of heavy projectiles from the ionic centers of a crystal surface. The work is focused on the process of electron capture at intermediate and high impact velocities. Within the impact-parameter formalism we extend the use of the eikonal-impulse (EI) approximation [14] to deal with a large collection atoms or ionic centers. The EI approximation is a distorted wave method that makes use of the eikonal wave function in the initial channel and the exact impulse wave function in the final channel. This theory has proved appropriate to explain charge exchange processes for a large variety of collision systems [14,15].

The method is applied to grazing protons impinging on a LiF(100) surface, which is an insulator material. We found that under surface channeling conditions, the electron transfer probability from a given initial state within the band structure displays sharp maximums in preferential directions. These preferential axes do not necessarily coincide with low-index crystallographic directions, and their orientations depend on the transferred electron momentum.

Notably, when the contributions coming from different crystal states are added to obtain the total capture probability from the surface band, the interference effects almost completely disappear. In this way, the total transition probability for the coherent process tends to the value corresponding to random incidence, usually known as the incoherent probability.

The article is organized as follows. In Sec. II we present the theoretical model used to calculate coherent electron capture. In Sec. III results are shown and discussed, and Sec. IV contains our conclusions. Atomic units are used unless otherwise stated.

II. THEORETICAL MODEL

A heavy projectile (P) of charge z_P and mass M_P impinges grazingly on an orthorhombic crystal surface (S). As a consequence of the collision, an electron (e) initially bound to the crystal in the surface band i is transferred to the final state f bound to the projectile. The frame of reference is fixed on a target nucleus belonging to the first atomic layer, with the $\hat{z}$ versor perpendicular to surface plane and the $\hat{x}$ and $\hat{y}$ versors coinciding with the lattice axis, as indicated in Fig. 1.

Within the impact-parameter formalism the motion of the projectile is described in terms of its classical trajectory. For grazing collisions the path of the incident ion can be divided into differential portions situated at different distances Z from the surface. At every portion the component of the projectile velocity perpendicular to the surface is considered negligible, and the ion moves parallel to the surface plane with velocity $\vec{v}=(v\cos\theta, v\sin\theta, 0)$, v being the incidence velocity, which is constant. The angle θ determines the orientation of the projectile trajectory with respect to the crystal axes; i.e., θ is the angle formed by the scattering plane and the $\hat{x}$ versor.

The position of the projectile at a given time t reads

$$\vec{R}(t) = \vec{R}_0 + Z(\xi)\hat{z} + \vec{v}t, \tag{1}$$

where $Z(\xi)$ is the classical ion path, $\xi = vt$ is the coordinate of the projectile along the direction of $\vec{v}$, and $\vec{R}_0 + Z(0)\hat{z}$

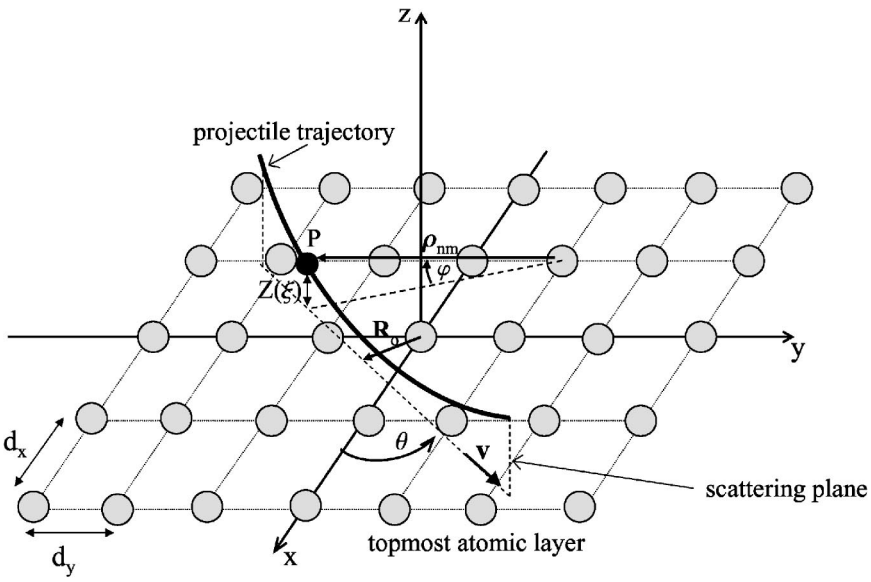

FIG. 1. Schematic depiction of the coordinate system.

$=(X_0, Y_0, Z(0))$ denotes the position of maximum approach to the surface (see Fig. 1).

To describe the electron transfer process we employ the independent electron model, in which noncaptured electrons remain frozen in their initial states. In this way the problem is reduced to a one-active-electron system [16]. The electronic state $\Psi_i^+(t)$ associated with the collision satisfies the time-dependent Schrödinger equation for the Hamiltonian

$$H(t) = h_s + V_{Pe}(\vec{r}_P(t)), \tag{2}$$

with

$$h_s = -\frac{1}{2}\nabla_{\vec{r}}^2 + V_{Se}(\vec{r}) \tag{3}$$

the crystal Hamiltonian, where $\vec{r}$ is the position vector of the active electron e, $\vec{r}_P(t)=\vec{r}-\vec{R}(t)$ denotes the position of e with respect to the projectile, and the potentials $V_{Pe}(\vec{r}_P) = -z_P/|\vec{r}_P|$ and V_{Se} represent the e-P and e-S interactions, respectively. As initial condition, when $t\to-\infty$ the state $\Psi_i^+(t)$ tends to the unperturbed state $\Phi_i(t)=\exp(-i\epsilon_i t)\phi_i$, where ϕ_i is eigenfunction of h_s with energy ϵ_i.

In insulator surfaces electrons are strongly localized around the atoms or ionic centers of the crystal lattice. Therefore, only those electrons bound to atoms situated at the first atomic plane contribute effectively to the electron capture. Using the Bloch representation the initial unperturbed state ϕ_i is expressed as [17]

$$\phi_i \equiv \phi_{i\vec{k}}(\vec{r}) = \sum_{n,m=-\infty}^{\infty} e^{i\vec{k}\cdot\vec{x}_{nm}}\, \varphi_i(\vec{r}-\vec{x}_{nm}), \tag{4}$$

where the wave vector $\vec{k}=k_x\hat{x}+k_y\hat{y}\equiv(k_x,k_y)$ has been introduced to identify a given crystal state within the surface band i, with $\vec{k}$ belonging to the first Brillouin zone. In Eq. (4) the function φ_i represents a Wannier function and the position vectors

$$\vec{x}_{nm} = nd_x\hat{x} + md_y\hat{y}, \tag{5}$$

with $n,m=0,\pm1,\pm2,\ldots$, determine lattice sites corresponding to surface atoms, d_x and d_y being the shortest interatomic distances in the directions $\hat{x}$ and $\hat{y}$, respectively (see Fig. 1).

As a first estimation we consider that the overlap between wave functions corresponding to nearest-neighbor atoms is small, and the Wannier function φ_i approximates to the atomic wave function. The Bloch energy ϵ_i corresponding to $\phi_{i\vec{k}}$ can be roughly expressed as [17]

$$\epsilon_i \equiv \epsilon_i(\vec{k}) = \varepsilon_i - \frac{\delta_i}{2}\cos(k_x d_x)\cos(k_y d_y), \tag{6}$$

where ε_i is the eigenenergy associated with the atomic state φ_i and δ_i is the bandwidth.

A. Coherent transition amplitude

In this work we use a distorted-wave method—the EI theory—to describe the electronic transition $\phi_{i\vec{k}}\to\varphi_f$, φ_f being the final wave function bound to the projectile. The prior form of the EI transition amplitude reads [14,18]

$$A_{i\vec{k}} = -i\int_{-\infty}^{+\infty} dt\langle\chi_f^{I-}|V_f^{\dagger}|\chi_{i\vec{k}}^{E+}\rangle, \tag{7}$$

where $\chi_{i\vec{k}}^{E+}$ and χ_f^{I-} are the eikonal and exact impulse wave functions in the entrance and exit channels, respectively, and the sign $\pm$ indicates the incoming $(-)$ and outgoing $(+)$ asymptotic conditions. The potential V_f represents the perturbation in the final channel, which is given by $V_f|\chi_f^{I-}\rangle = [H(t)-id/dt]|\chi_f^{I-}\rangle$. For the considered collisional system, the initial eikonal wave function reads

$$\chi_{i\vec{k}}^{E+} = \phi_{i\vec{k}}(\vec{r})\exp[-i\epsilon_i(\vec{k})t]E^+(z_P,-\vec{v},\vec{r}_P), \tag{8}$$

where $E^+(z_P,-\vec{v},\vec{r}_P)=\exp[-iz_P/v\,\ln(vr_P+\vec{v}\cdot\vec{r}_P)]$ is the eikonal phase that describes the asymptotic distortion produced by the projectile in the entrance channel, with $r_P=|\vec{r}_P|$. The final exact impulse wave function reads

$$\chi_f^{I-} = \frac{1}{(2\pi)^{3/2}} \int d\vec{q}\,\tilde{\varphi}_f(\vec{q})\exp(i\vec{q}\cdot\vec{r}_P)\mathcal{D}_S^-(\vec{q}+\vec{v},\vec{r}) \times \exp(-i\varepsilon_f t)\exp(i\vec{v}\cdot\vec{r} - iv^2 t/2), \tag{9}$$

where the function $\mathcal{D}_S^-(\vec{p},\vec{r})$ represents the distortion introduced by the crystal surface in the exit channel and the tilde denotes the Fourier transform. In Eq. (9), ε_f is the eigenenergy associated with the final state φ_f and the last exponential factor (translation factor) takes into account that the projectile is moving in the frame of reference [19].

Replacing Eqs. (8) and (9) in Eq. (7) the coherent transition amplitude, except for a constant phase, reads

$$A_{i\vec{k}} = \sum_{n,m=-\infty}^{\infty} \exp[i(\vec{k}-\vec{W})\cdot\vec{x}_{nm}]\mathcal{A}_i^{(n,m)}, \tag{10}$$

where

$$\mathcal{A}_i^{(n,m)} = \int_{-\infty}^{+\infty} dt' \exp[i(\vec{v}-\vec{W})\cdot\vec{v}t'] \int d\vec{q}\,\tilde{\varphi}_f^*(\vec{q}) \times \int d\vec{r}\frac{\exp[-i(\vec{v}\cdot\vec{r}_{nm}+\vec{q}\cdot\vec{r}_P)]}{(2\pi)^{3/2}}\varphi_i(\vec{r}_{nm}) \times \mathcal{D}_S^{-*}(\vec{q}+\vec{v},\vec{r})\Delta(\vec{q},\vec{r}_P)E^+(z_P,-\vec{v},\vec{r}_P), \tag{11}$$

with $\vec{r}_{nm}=\vec{r}-\vec{x}_{nm}$ and $\Delta(\vec{q},\vec{r}_P)=q^2/2-\varepsilon_f+V_{Pe}(\vec{r}_P)$. The vector

$$\vec{W} = \left(\frac{v}{2} + \frac{\epsilon_i(\vec{k})-\varepsilon_f}{v}\right)\hat{v} \tag{12}$$

is the transferred momentum vector parallel to $\hat{v}$, with $\hat{v}=\vec{v}/v$. Note that in every term of Eq. (10) the integration variable t has been changed by the variable t', which fixes the time origin when the projectile is at the closest distance from the $\vec{x}_{nm}$ site, as expressed in Eq. (11).

The function $\mathcal{A}_i^{(n,m)}$, given by Eq. (11), is related to the capture from the atomic bound state $\varphi_i(\vec{r}_{nm})$, which is centered around the position $\vec{x}_{nm}$ of the lattice. We assume that when the electron e is captured from a region close to the $\vec{x}_{nm}$ site, what happens is the following.

(i) In the exit channel, the charge of passive electrons fully screens the other ionic centers, and the final interaction between e and the ionic core placed at the position $\vec{x}_{nm}$ can be represented by a Coulomb potential with effective charge z_T. Then, in Eq. (11) we replace the function $\mathcal{D}_S^-(\vec{p},\vec{r})$ by the Coulomb distortion factor $D^-(z_T,\vec{p},\vec{r}_{nm})=\exp[\pi z_T/(2p)]\Gamma(1+iz_T/p)_1F_1(-iz_T/p,1,-ipr_{nm}-i\vec{p}\cdot\vec{r}_{nm})$, with ${}_1F_1$ the confluent hypergeometric function and $p=|\vec{p}|$.

(ii) Only the time interval in which the projectile moves close to the position $\vec{x}_{nm}$ contributes effectively to the transition amplitude. Consequently, the position vector of the projectile can be approximated by

$$\vec{R}(t') = \vec{x}_{nm} + \vec{\rho}_{nm} + \vec{v}t', \tag{13}$$

where $\vec{\rho}_{nm}$ denotes the impact parameter measured with respect to site $\vec{x}_{nm}$, with $\vec{\rho}_{nm}\cdot\vec{v}=0$. According to geometry, the impact parameter is expressed as $\vec{\rho}_{nm}=-\zeta_{nm}\hat{u}+Z(\xi_{nm})\hat{z}$, where $\vec{x}_{nm}-\vec{R}_0=\xi_{nm}\hat{v}+\zeta_{nm}\hat{u}$ and $\hat{u}=\hat{z}\times\hat{v}$.

Taking into account the assumptions (i) and (ii), from Eq. (11) we can derive a partial transition matrix $T_i^{(n,m)}$ by using the usual eikonal transformation [19]—that is, $T_i^{(n,m)}(\vec{\eta}) = v/(2\pi)^3 \int d\vec{\rho}_{nm}\mathcal{A}_i^{(n,m)}\exp(-i\vec{\eta}\cdot\vec{\rho}_{nm})$, where $\vec{\eta}$ is the perpendicular transferred momentum, with $\vec{\eta}\cdot\vec{v}=0$. After some algebra, the transition matrix $T_i^{(n,m)}$ becomes independent of the particular lattice site $\vec{x}_{nm}$, and it reads

$$T_i(\vec{\eta}) = \frac{1}{(2\pi)^{3/2}} \int d\vec{q}\,\tilde{\varphi}_f^*(\vec{q})L_{Ti}^{-*}(\vec{q}+\vec{v},-\vec{W}_T) \times \left[\left(\frac{q^2}{2}-\varepsilon_f\right)I_P^+(-\vec{v},\vec{q}+\vec{W}_P) + J_P^+(-\vec{v},\vec{q}+\vec{W}_P)\right], \tag{14}$$

where we have explicitly omitted the (n,m) supraindex. The auxiliary functions

$$\begin{Bmatrix} I_P^+(\vec{p},\vec{q}) \\ J_P^+(\vec{p},\vec{q}) \end{Bmatrix} = \int d\vec{r}\frac{\exp(-i\vec{q}\cdot\vec{r})}{(2\pi)^{3/2}} \times \begin{Bmatrix} 1 \\ V_{Pe}(\vec{r}) \end{Bmatrix} \times E^+(z_P,\vec{p},\vec{r}) \tag{15}$$

and

$$L_{Ti}^-(\vec{p},\vec{q}) = \int d\vec{r}\frac{\exp(-i\vec{q}\cdot\vec{r})}{(2\pi)^{3/2}}\varphi_i^*(\vec{r})D^-(z_T,\vec{p},\vec{r}) \tag{16}$$

are Nordsieck-type integrals, which have closed forms [20], and $\vec{W}_T=\vec{\eta}+\vec{W}$ and $\vec{W}_P=\vec{v}-\vec{W}_T$ are the well-known transferred momentum vectors.

The function $T_i(\vec{\eta})$, given Eq. (14), coincides with the transition matrix corresponding to electron capture from the atomic bound state φ_i. By employing the eikonal relation once more [19] we obtain $\mathcal{A}_i^{(n,m)}=a_i^{(at)}(\vec{\rho}_{nm})$, where

$$a_i^{(at)}(\vec{\rho}) = \frac{2\pi}{v}\int d\vec{\eta}\; T_i(\vec{\eta})\exp(i\vec{\eta}\cdot\vec{\rho}) \tag{17}$$

represents the amplitude for the atomic transition $\varphi_i \to \varphi_f$ and all information about the particular lattice site from which the electron is captured is contained in the impact parameter $\vec{\rho}_{nm}$. Replacing this expression in Eq. (10), the coherent transition amplitude reads

$$A_{i\vec{k}} = \sum_{n,m=-\infty}^{\infty} \exp[i(\vec{k}-\vec{W})\cdot\vec{x}_{nm}]a_i^{(at)}(\vec{\rho}_{nm}). \tag{18}$$

Therefore, the coherent process of electron transfer from the crystal surface looks like a collection of individual atomic captures, each of them from a different lattice site $\vec{x}_{nm}$.

B. Partial and total capture probabilities

The electron capture probability from a given crystal state $\phi_{i\vec{k}}$ within the surface band i is derived from Eq. (18) as

$$P_{i\vec{k}} = \frac{1}{S_0}\int_{S_0} d\vec{R}_0|A_{i\vec{k}}|^2, \tag{19}$$

where the integral on $\vec{R}_0$ has been introduced to average the different positions around the origin where the projectile can

reach the closest distance to the surface and S_0, chosen as $S_0 = d_x d_y$, denotes the integration area. The probability $P_{i\vec{k}}$ given by Eq. (19) will be here named partial capture probability, in contrast with the total capture probability from the surface band i, denoted as P_i.

The total probability P_i is obtained by adding the partial probabilities $P_{i\vec{k}}$ for the different initial crystal states—that is,

$$P_i = \frac{1}{\mathcal{S}} \int_{\mathcal{S}} d\vec{k}\, P_{i\vec{k}}, \tag{20}$$

where $\mathcal{S}$ refers to the area of the first Brillouin zone, $\mathcal{S} = (2\pi)^2/S$, with S the surface of the primitive cell of the direct lattice [17].

Incoherent limit

Replacing Eq. (18) in Eq. (19) the total capture probability P_i reads

$$P_i = \sum_{n',m'} \sum_{n,m} \int_{\mathcal{S}} \frac{d\vec{k}}{\mathcal{S}} \exp[i(\vec{k} - \vec{W}) \cdot (\vec{x}_{nm} - \vec{x}_{n'm'})] \times \int_{S_0} \frac{d\vec{R}_0}{S_0} a_i^{(at)}(\vec{\rho}_{nm}) a_i^{(at)^*}(\vec{\rho}_{n'm'}). \tag{21}$$

Note that even though the $\vec{k}$ dependence has not been explicitly included, the integrand of Eq. (21) also depends on $\vec{k}$ through the transferred momentum $\vec{W}$, as indicated by Eq. (12). However, for high impact velocities the momentum $\vec{W}$ varies only slightly with $\vec{k}$, and it can be considered a constant. Under this assumption the integral on $\vec{k}$ in Eq. (21) can be analytically solved, and the total capture probability from the surface band i approximates to

$$P_i \approx \int_{S_0} \frac{d\vec{R}_0}{S_0} \sum_{n,m} |a_i^{(at)}(\vec{\rho}_{nm})|^2. \tag{22}$$

By changing the sum on the discrete indexes (n,m) that identify the different lattice site by an integral on the surface plane, we find that P_i tends to the incoherent value corresponding to random incidence [21]. That is, $P_i \approx P_i^{(in)}$, with

$$P_i^{(in)} = \lambda_s \int d\vec{x}'\; P_i^{(at)}(\vec{\rho}(\vec{x}')), \tag{23}$$

where $P_i^{(at)}(\vec{\rho}) = |a_i^{(at)}(\vec{\rho})|^2$ is the atomic capture probability from the initial state φ_i as a function of the impact parameter $\vec{\rho}$ and λ_s is the surface atomic density, which depends on the Miller indices of the crystallographic surface. In Eq. (23) the impact parameter $\vec{\rho}$ depends on the position on the surface plane $\vec{x}' = (x', y', 0)$,

$$\rho(x', y') = \sqrt{y'^2 + Z^2(x')}, \quad \varphi(x', y') = \arctan\left(\frac{Z(x')}{y'}\right), \tag{24}$$

being the modulus and the azimuthal angle, respectively, of $\vec{\rho}$.

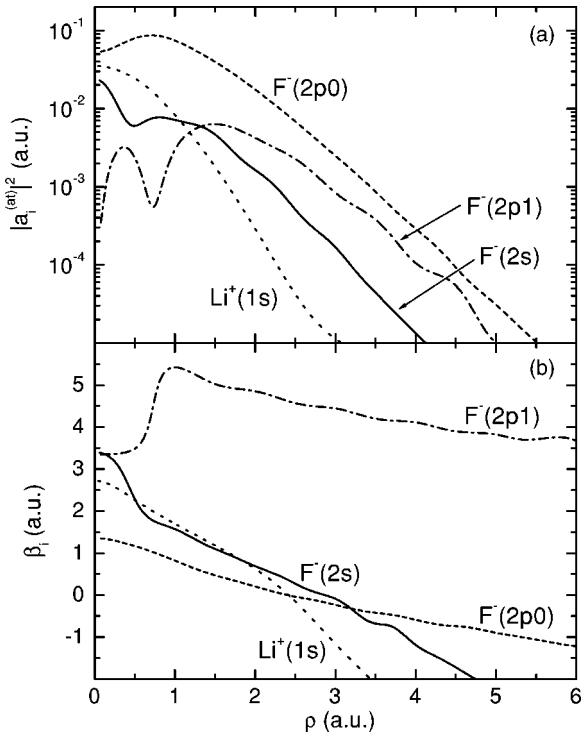

FIG. 2. Module and phase of the atomic transition amplitude $a_i^{(at)}$ as a function of the impact parameter ρ for 100 keV protons impinging on Li^+ and F^- ions. (a) Atomic capture probability $P_i^{(at)} = |a_i^{(at)}|^2$ and (b) phase β_i of $a_i^{(at)}$ as defined by Eq. (25). Dotted line: capture from the 1*s* state of lithium. Solid, dashed, and dash-dotted lines: capture from states 2*s*, $2p_0$, and $2p_1$ of fluor, respectively.

III. RESULTS

Our study has concentrated on 100 keV protons impinging on a LiF(100) surface with the angle of incidence $\theta_i = 0.7°$, which is measured with respect to the surface plane [22]. The LiF can be considered as the typical example of orthorhombic ionic crystal: valence electrons are localized around ionic centers, placed at sites of a cubic lattice, with $d_x = d_y = 3.8$ a.u. For this collisional system, proton neutralization is principally caused by the electron transfer to the ground state of hydrogen from bound states to surface ions. We evaluated the electron exchange processes from the K shell of Li^+ cations and the L shell of F^- anions using the standard EI approximation [14]. The K shell of F^- is not included in our calculations because its contribution is negligible at the considered impact energy. The wave functions φ_i corresponding to Li^+ and F^- ions were represented by Hartree-Fock wave functions for positive and negative ions [23], respectively. No correction was included in φ_i to take into account the interaction of the target ion with nearest neighbors. By using energy requirements, we chose the effective charge z_T as $z_T = \sqrt{-2n_i^2 \varepsilon_i}$ [24,25], where n_i is the principal quantum number associated with φ_i and ε_i is its eigenenergy. The 2*s* and 2*p* bandwidths of fluor were estimated as 1.6 and 5.0 eV, respectively [26,27], and the bandwidth corresponding to the state 1*s* of lithium was neglected.

For every initial state, the calculation of the transition matrix T_i involves a three-dimensional integration on the

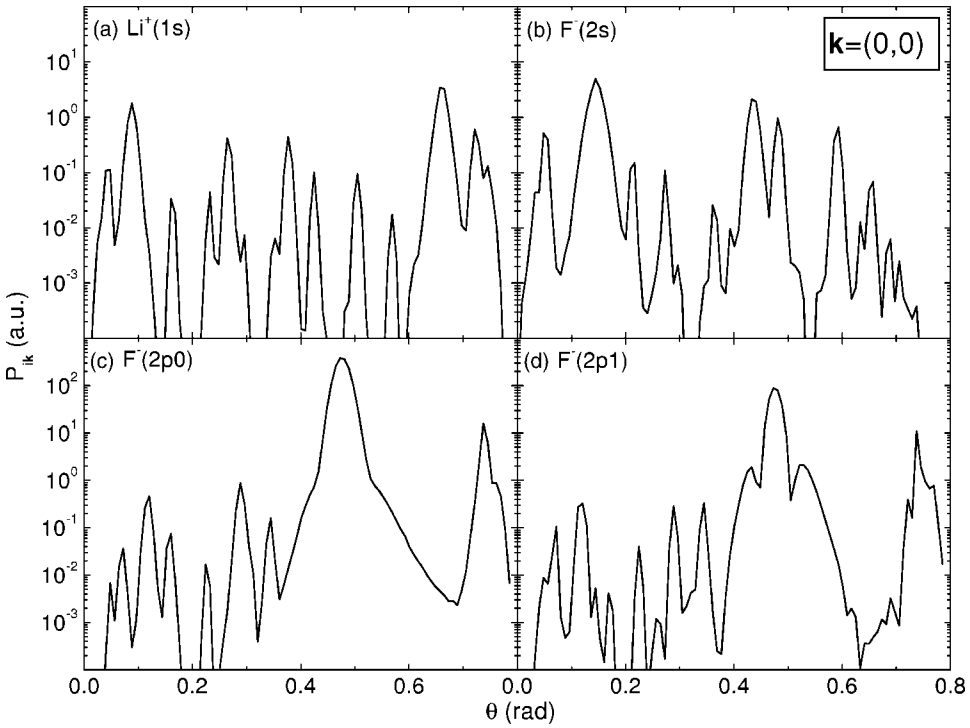

FIG. 3. Partial capture probabilities $P_{i\vec{k}}$ from initial crystal states with $\vec{k}=(0,0)$, as given by Eq. (19), as a function of the orientation angle of the trajectory, θ. The collision system is composed of 100 keV protons impinging on a LiF(100) surface with the incidence angle $\theta_i=0.7°$. The following surface bands were considered: (a) $Li^+(1s)$, (b) $F^-(2s)$, (c) $F^-(2p_0)$, and (d) $F^-(2p_1)$.

variable $\vec{q}$ [Eq. (14)], which was numerically evaluated with a relative error lower than 1%. The further numerical integration on $\vec{\eta}$, involved in Eq. (17), was done with an relative error of 1%. To evaluate the infinite sum on the lattice sites contained in Eq. (18) we considered about 500 sites along the projectile path and approximately 10 sites in the direction perpendicular to $\vec{v}$. The additional integrations on the variables $\vec{R}_0$ and $\vec{k}$ involved in Eqs. (19) and (20), respectively, were done with the Monte Carlo numerical technique, with an error lower than 5%. The classical trajectory of the projectile, $Z(\xi)$, was determined employing the Ziegler-Biersack-Littmark (ZBL) potential [28] to describe the projectile-surface interaction.

To derive the coherent transition amplitude, as given by Eq. (18), it is necessary to take into account not only the modulus but also the phase of the atomic transition amplitude $a_i^{(at)}$. Including the internuclear projectile-target potential by means of the eikonal treatment, the transition amplitude $a_i^{(at)}$ reads [24]

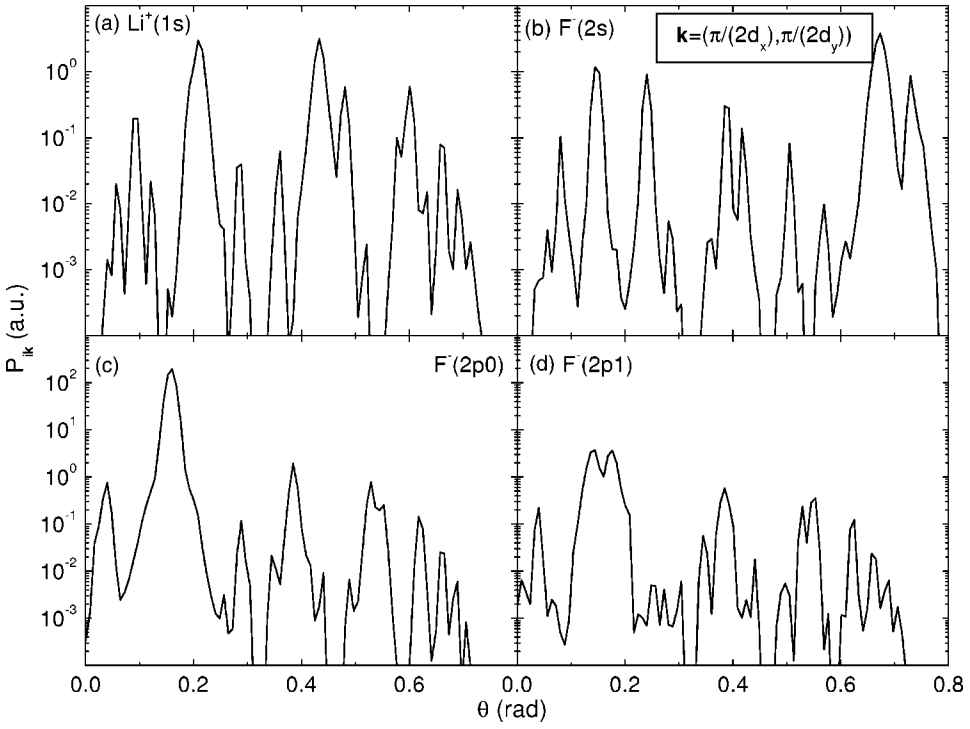

FIG. 4. Similar to Fig. 3 for initial crystal states with $\vec{k}=(\pi/(2d_x),\pi/(2d_y))$.

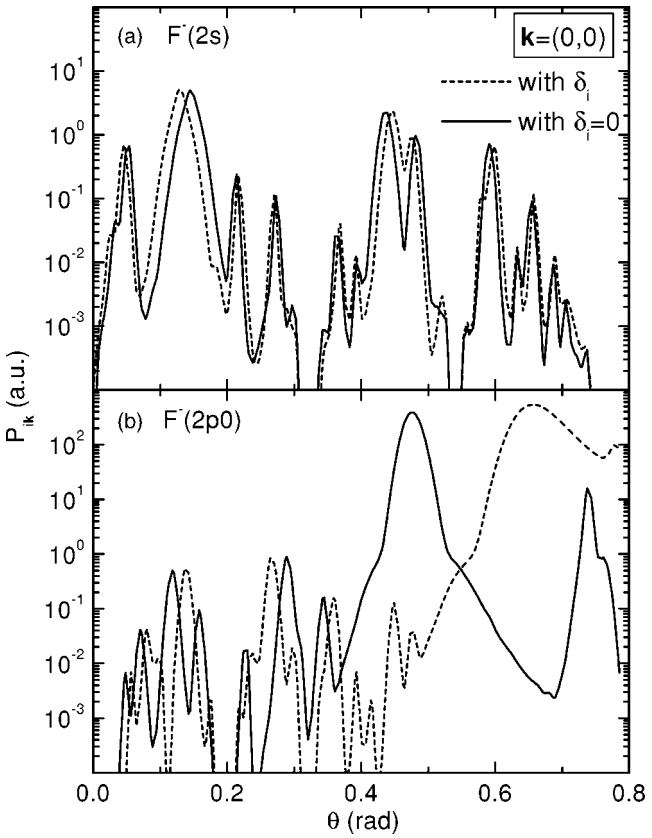

FIG. 5. Similar to Fig. 3 for the surface bands (a) $F^-(2s)$ and (b) $F^-(2p_0)$. Solid lines: results including the bandwidth δ_i as given by Eq. (6). Dashed lines: results obtained by fixing $\delta_i=0$.

$$a_i^{(at)}(\vec{\rho}) = |a_i^{(at)}(\rho)|\exp\left\{ i\left[\beta_i(\rho) + (m_i - m_f)\varphi - \nu_{TP} \ln\left(\frac{2v}{\rho}\right)\right]\right\}, \tag{25}$$

where $m_{i(f)}$ is the magnetic number corresponding to the initial (final) atomic state and $\nu_{TP}=2z_Tz_P/v$. The variables ρ and φ are the modulus and the azimuthal angle, respectively, of the impact parameter $\vec{\rho}$, and β_i represents the phase for $\varphi=0$, in the absence of the internuclear potential. In Fig. 2(a) we display the atomic capture probability $P_i^{(at)}=|a_i^{(at)}|^2$, as a function of the modulus of the impact parameter. In the whole range of considered impact parameters, captured electrons essentially come from the $F^-(2p_0)$ state. The contribution from the state $Li^+(1s)$ is important only for small values of ρ, decreasing strongly for $\rho>1$ a.u. The phase β_i of the atomic transition amplitude is shown in Fig. 2(b) as a function of ρ, for the different initial states. In all cases, β_i smoothly decreases as ρ increases.

Partial capture probabilities from initial crystal states with $\vec{k}=(0,0)$ are displayed in Fig. 3 for the surface bands $Li^+(1s)$, $F^-(2s)$, $F^-(2p_0)$, and $F^-(2p_1)$, respectively. They are plotted as a function of the angle θ that determines the orientation of the projectile trajectory with respect to the crystal axes. As a result of the symmetry of the problem, only θ values ranging from 0 to $\pi/4$ are shown. Strong interference effects are observed in Fig. 3; there are preferential directions of the crystal along which surface capture probability $P_{i\vec{k}}$ presents sharp maxima, while for other directions the process is almost completely suppressed. The orientation of these directions varies with the considered surface band. As the modulus and phase of $a_i^{(at)}$ vary smoothly with ρ, from Eq. (18) the maxima of $P_{i\vec{k}}$ roughly correspond to scattering along surface-ion strings that verify $(\vec{k}\cdot\hat{v}-W)d\simeq N2\pi$, d being the spacing between adjacent ions of the string and N small integer numbers. Therefore, the set of angles θ for which the capture probability displays maxima is different for every initial band i because the transferred momentum W depends on the Bloch energy $\epsilon_i(\vec{k})$. For LiF surfaces, equal probabilities are obtained for initial states with $\vec{k}=\pm(\pi/d_x,\pi/d_y)$ due to Li^+ and F^- ions occupy alternative lattice sites and, consequently, phases $[(\vec{k}-\vec{W})\cdot\vec{x}_{nm}]$ differ only in integers times 2π with respect to $\vec{k}=(0,0)$. In Fig. 4 we show partial capture probabilities from initial states with $\vec{k}=(\pi/(2d_x),\pi/(2d_y))$, again for the surface bands $Li^+(1s)$, $F^-(2s)$, $F^-(2p_0)$, and $F^-(2p_1)$. For this value of $\vec{k}$ different interference patterns are obtained in comparison with those displayed in Fig. 3.

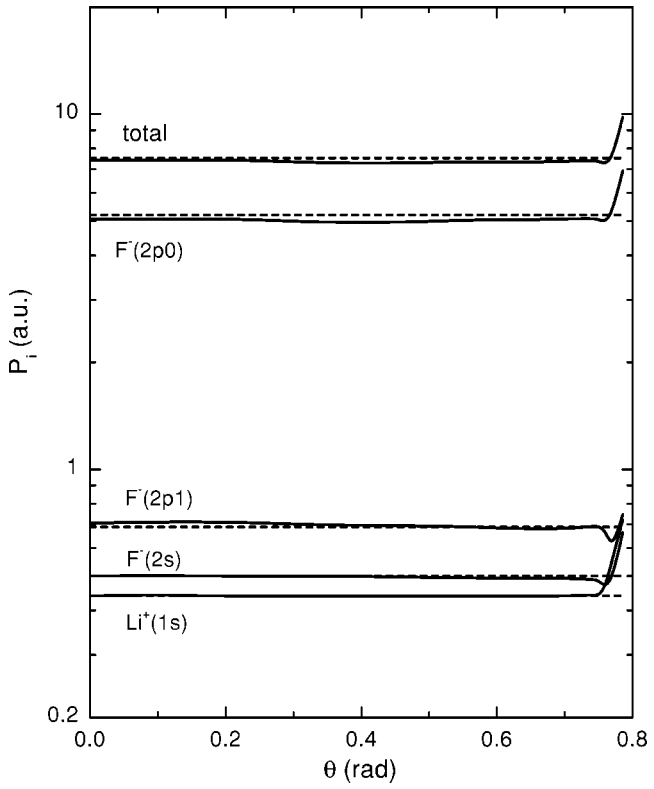

FIG. 6. Total capture probability from the surface bands $Li^+(1s)$, $F^-(2s)$, $F^-(2p^0)$, and $F^-(2p_1)$ as a function of the orientation angle θ. Solid line: coherent probability P_i, as given by Eq. (20). Dashed line: incoherent probability $P_i^{(in)}$, as given by Eq. (23).

To investigate the dependency of these interference structures with the bandwidth δ_i, in Fig. 5 we display capture probabilities $P_{i\vec{k}}$ derived by fixing $\delta_i=0$, comparing the results with those obtained by including the energy dispersion

δ_i. Initial states with $\vec{k}=(0,0)$ within the bands $F^-(2s)$ and $F^-(2p_0)$ are considered. While for the $2s$ band the shift introduced by δ_i is small, for the $2p$ band not only the position of the maxima but also the shape of the curve changes by neglecting δ_i, especially at large θ angles. We estimate that for the $F^-(2p)$ band a more precise determination of the Bloch energy could modify the interference patterns here obtained. These patterns could be experimentally observed by measuring the electron capture process in coincidence with the filling of the $\vec{k}$ vacancy. Such experiments would allow one to study the properties of the crystal states. As the coherent sum involved in Eq. (18) strongly depends of the distance between surface ions, we also analyzed the effects produced by thermal vibrations of the lattice, and they were found to be small at normal temperatures.

Total capture probabilities from the surface bands $2s$, $2p_0$, and $2p_1$ of fluor anions and $1s$ of lithium cations are plotted in Fig. 6 as a function the angle θ. These probabilities were obtained by adding contributions coming from different crystal states $\phi_{i\vec{k}}$, as indicated in Eq. (20). Remarkably, the interference effects produced by the coherent capture from different lattice sites disappear when the total probability is considered. The total results obtained from Eq. (20) coincide quite well with the incoherent values, derived from Eq. (23), except for θ close to $\pi/4$, where a small increment of P_i seems to remain as a signature of the interference. This holds even for the bands $F^-(2p)$ for which the effect of the bandwidth is large. For the incidence angle $\theta_i=0.7°$ the incoherent capture probabilities are 0.44, 0.50, 5.20, and 0.69 a.u. for the bands $Li^+(1s)$, $F^-(2s)$, $F^-(2p_0)$, and $F^-(2p_1)$, respectively. It should be noted that for a given $\vec{k}$ value, the average on the angle θ of $P_{i\vec{k}}$ does not lead to the incoherent probability, associated with random incidence. The partial probability $P_{i\vec{k}}$ roughly reaches the incoherent limit only if the phase $\beta_i(\rho)$ is taken as a random number and the number of atomic collisions is increased from 500 to more than 4000 by decreasing the interatomic distances d_x and d_y.

IV. CONCLUSIONS

In the present work, the electron transfer process by the grazing incidence of ions on solid surfaces has been studied at high impact energies. Employing a distorted-wave method—the EI approximation—we have expressed the transition amplitude for coherent electron capture from the surface as a sum of atomic transition amplitudes, each of them associated with electron transfer from only one lattice site. We have found that for a given initial crystal state, the capture probability exhibits maxima and minima related to scattering along preferential directions. These preferential axes do not necessarily coincide with low-index crystallographic directions, and they vary with the crystal state considered.

The interference patterns almost completely disappear when the contributions from different crystal states are added to obtain the total capture probability from the surface band. The total transition probability for the coherent process tends to the value corresponding to random incidence, usually known as incoherent probability, and only a weak interference effect is observed for the angle $\theta\approx\pi/4$. Although more precise calculations should be necessary to confirm these findings, we expect that under axial surface channeling conditions, accurate measurement of the energy and charge state of the ion will allow to observe interference structures. Similar effects should be also found at lower impact velocities, where interferences patterns could be enhanced for surface bands with a large bandwidth. In slow collisions, coherence phenomena could also affect the probability of the formation of negative hydrogen ions, which are considered as a precursor for the electron-emission process [29]. As a future development, we plan to introduce into the model a surface interaction that takes into account the crystallographic orientation [30] to describe channeling projectile trajectories.

ACKNOWLEDGMENTS

Financial support from the ANPCyT (Grant Nos. PICT 99-0306249 and PICTR 02-00122), CONICET (Grant No. PIP 657), and UBACyT (Grant No. 03-X259) is acknowledged and greatly valued.

[1] K. Kimura, H. Ida, M. Fritz, and H. Mannami, Phys. Rev. Lett. **76**, 3850 (1996).
[2] C. Auth, A. Mertens, H. Winter, A. G. Borisov, and F. J. García de Abajo, Phys. Rev. Lett. **79**, 4477 (1997).
[3] F. J. García de Abajo, V. H. Ponce, and P. M. Echenique, Phys. Rev. Lett. **69**, 2364 (1992).
[4] F. J. García de Abajo, Nucl. Instrum. Methods Phys. Res. B **125**, 1 (1997).
[5] S. Datz *et al.*, Phys. Rev. Lett. **40**, 843 (1978).
[6] S. Datz *et al.*, Nucl. Instrum. Methods **170**, 15 (1980).
[7] H. F. Krause *et al.*, Phys. Rev. Lett. **71**, 348 (1993).
[8] K. Kimura *et al.*, Phys. Rev. Lett. **66**, 25 (1991).
[9] F. Fujimoto *et al.*, Nucl. Instrum. Methods Phys. Res. B **33**, 354 (1988).
[10] S. Datz *et al.*, Nucl. Instrum. Methods Phys. Res. B **100**, 272 (1995).
[11] N. Stolterfoht *et al.*, Phys. Rev. Lett. **87**, 023201 (2001).
[12] M. E. Galassi, R. D. Rivarola, P. D. Fainstein, and N. Stolterfoht, Phys. Rev. A **66**, 052705 (2002).
[13] N. Stolterfoht *et al.*, Phys. Rev. A **69**, 012701 (2004).
[14] M. S. Gravielle and J. E. Miraglia, Phys. Rev. A **44**, 7299 (1991).
[15] M. S. Gravielle and J. E. Miraglia, Phys. Rev. A **51**, 2131 (1995).
[16] H. F. Busnengo, S. E. Corchs, and R. D. Rivarola, Phys. Rev. A **57**, 2701 (1998).
[17] N. W. Ashcroft and N. D. Mermin, *Solid State Physics* (Holt, Rinehart and Winston, New York, 1976).

[18] D. P. Dewangan and J. Eichler, Phys. Rep. **247**, 59 (1994).
[19] M. R. C. McDowell and J. P. Coleman, *Introduction to the Theory of Ion-Atom Collisions* (North-Holland, Amsterdam, 1970).
[20] M. S. Gravielle and J. E. Miraglia, Comput. Phys. Commun. **69**, 53 (1992).
[21] M. S. Gravielle and J. E. Miraglia, Phys. Rev. A **50**, 2425 (1994).
[22] G. R. Gomez, O. Grizzi, E. A. Sanchez, and V. H. Ponce, Phys. Rev. B **58**, 7403 (1998).
[23] E. Clementi and C. Roetti, At. Data Nucl. Data Tables **14**, 177 (1974).
[24] Dz. Belkic, R. Gayet, and A. Salin, Phys. Rep. **56**, 279 (1979).
[25] P. N. Abufager, A. E. Martínez, R. D. Rivarola, and P. D. Fainstein, J. Phys. B **37**, 817 (2004).
[26] A. Arnau (private communication).
[27] Theoretical bandwidths were corrected by a factor of 1.6 to fit experimental values.
[28] J. F. Ziegler, J. P. Biersack, and U. Littmark, in *The Stopping and Range of Ions in Matter*, edited by J. F. Ziegler (Pergamon, New York, 1985), Vol. 1.
[29] H. Winter, A. Mertens, S. Lederer, C. Auth, F. Aumayr, and H. P. Winter, Nucl. Instrum. Methods Phys. Res. B **212**, 45 (2003).
[30] A. Schüller, G. Adamov, S. Wethekam, K. Maass, A. Mertens, and H. Winter, Phys. Rev. A **69**, 050901 (2004).